Int. J. Electrochem. Sci., 17 **(2022)** Article Number: 221278, doi: 10.20964/2022.12.61

International Journal of
ELECTROCHEMICAL
SCIENCE
www.electrochemsci.org

Short Communication

Evaluation of Corrosion Resistance of Steel Reinforced Concrete Containing Ordinary Portland Cement Blended with Wheat Ash and Blast Furnace Slags as Mineral Admixture Under Simulated Marine Condition

Mingming Liu[1], *Kangning Liu*[2,*] *Bo Liu*[3]

[1] School of Civil Engineering, Xijing University, Xi'an 710123, PR China
[2] School of Civil Engineering, Xi'an University of Architecture & Technology, Xi'an 710055, PR China
[3] China Railway 20th Bureau Group Co. Ltd., Xi'an 710016, China
[*]E-mail: Lkn09876@sina.com

Received: 20 October 2022 / *Accepted:* 29 November 2022 / *Published:* 27 December 2022

Current study was conducted on the evaluation of corrosion resistance of reinforced concrete containing ordinary Portland cement (OPC) blended with wheat ash (WA) and wheat stalk ash (BFS) as mineral admixtures under simulated marine conditions using electrochemical techniques. WA and BFS admixtures were used to partially replace the OPC including OPC0 as control sample (400 kg/m^3 OPC), OPC+BFS60 (340 kg/m^3 OPC+60 kg/m^3 BFS), OPC+WA60 (340 kg/m^3 OPC + 60 kg/m^3 WA) and OPC+WA30+BFS30 (340 kg/m^3 OPC+30 kg/m^3 WA + 30 kg/m^3 BFS). Results of potentiodynamic polarization, cyclic voltammetry and electrochemical impedance spectroscopy analyses indicated that OPC+WA30+BFS30 sample showed higher corrosion resistance and potential than the other samples because of the synergetic effect BFS and WA in concrete which enhanced the steel rebar corrosion resistance in 3.5 wt% NaCl solution. Moreover, the SEM studies showed that the OPC+WA30+BFS30 had lower corrosion products and lower density of narrow pits on steel surface than that OPC0 specimen which confirmed the electrochemical studies. These results demonstrated that WA and BFS can used as appropriate mineral admixtures to decrease hydroxide ion concentrations and enhance the passivation of the reinforcement steel rebar in marine environments.

Keywords: Mineral Admixture; Reinforced Concrete; Wheat Stalk Ash, Blast Furnace, Portland cement; Corrosion Resistance, Electrochemical Technique

1. INTRODUCTION

Concrete is increasingly being used in the construction of structures to provide strength, durability, and versatility. Concrete's excellent properties have made it a dependable and long-lasting

choice of construction companies for both commercial and residential constructions [1]. Reinforced concrete is created by concealing steel reinforcement, known as rebar, within the concrete [2]. Reinforced concrete has greater overall strength than regular concrete, so it can support more weight over a longer time and has a longer service life with relatively low maintenance, thus a lower maintenance cost. However, steel reinforcement corrosion and extreme weather conditions are significant issues with reinforced concrete [3].

Mineral admixtures are any essentially insoluble material other than cement and aggregate used as a concrete ingredient and added to the batch immediately before or during mixing. Mineral admixtures include natural materials, processed natural materials, and artificial materials such as fly ash, slags, and silica fume which are typically added to concrete in more significant amounts to improve workability, resistance to thermal cracking, alkali-aggregate expansion, and sulfate attack, and to allow for a reduction in cement content [4, 5]. Because these mineral admixtures are byproducts of some industrial process that would otherwise be dumped into landfills, they are also environmentally friendly [6, 7]. In general, the benefits of mineral admixtures included lower costs, energy savings, improved workability, extensibility, and reduced alkali-aggregate reaction, increased water tightness, strength, and lower water demand [8, 9].

Among mineral admixtures, industrial and agricultural waste ashes such as blast furnace slags (BFS) and wheat ash (WA) can be eco-friendly and beneficial mineral additives because millions of tons are produced globally each year. As a result, numerous studies have been conducted to identify and optimize the level of agricultural waste ashes as admixtures in concrete [10, 11]. BFS as a nonmetallic compound is an intermediate product in conventional, coal-based steelmaking, it consists primarily of silicates, aluminosilicates, and calcium-alumina-silicates which shows the pozzolanic reactivity [12, 13]. The molten slag, which absorbs much sulfur from the charge, accounts for about 20% of iron production by mass. Furthermore, wheat straw contains 8.6% ash, with a silica content of 73%. Pozzolanic properties are present in both ashes burned at 570°C and 670°C [14, 15]. According to our best knowledge, this study is the first report on the evaluation of corrosion resistance of Portland cement blended with WA and blast BFS as mineral admixtures in reinforced concrete under simulated marine conditions.

2. EXPERIMENT

For preparation the concrete in current work, ordinary Portland cement (OPC, Jiangxi Yinshan White Cement Limited, China) was mixed with coarse and fine aggregates and water at room temperature. Table 1 shows the mineral admixture and cement's chemical properties. The wheat ash (WA, LiaoCheng, Shandong, China) and blast furnace slags (BFS, Liuzhou city, Guangxi, China) were used as cement replacement. The mixtures had 400 kg/m^3 binder content with adjusted water-to-cement ratio of 0.45. The composition of the different designs of mixtures is presented in Table 2. The resulting mixtures poured into the cylindrical shaped molds with a height of 25 cm and a diameter of 10 cm. The samples were maintained in curing at room temperature and relative humidity was 95% in airtight for 24 hours. Electrochemical measurements were performed using carbon steel rebar through 3.5 wt.% NaCl aqueous solution as the simulated marine environment for 60 days to evaluate the influence of WA

and BFS incorporations on corrosion resistance of reinforced concretes. The chemical composition of tested carbon steel is given in Table 3.

Table 1. Mineral admixture and cement's chemical properties in current study.

Properties	OPC	WA	BFS
CaO (%)	63.98	3.88	42.47
SiO_2 (%)	20.49	77.35	33.77
K_2O (%)	0.68	5.44	0.32
Al_2O_3 (%)	4.71	1.54	13.13
SO_3 (%)	2.95	0.11	0.15
MgO (%)	2.07	1.88	7.46
Fe_2O_3 (%)	2.99	1.27	0.49
Na_2O (%)	0.19	0.09	0.17
LOI	0.88	5.8	1.67

Table 2. The composition of the different designs of mixtures in current study.

Sample name	**OPC (kg/m^3)**	**Water (kg/m^3)**	**WA (kg/m^3)**	**BFS (kg/m^3)**	**Coarse aggregates (kg/m^3)**	**Fine aggregates (kg/m^3)**
OPC0	400	180	0	0	925	640
OPC + BFS60	340	180	0	60	890	625
OPC + WA60	340	180	60	0	890	625
OPC + WA30+BFS30	340	180	30	30	890	625

Table 3. The chemical composition of tested carbon steel rebar.

Chemical	**C**	**Mo**	**Sn**	**S**	**V**	**Ni**	**Mn**	**Cu**	**Si**	**N**	**Cr**	**Fe**
wt.%	0.21	0.02	0.02	0.01	0.05	0.06	1.31	0.26	0.18	0.01	0.09	residual

Electrochemical experiments using an electrochemical impedance spectroscopy (EIS) technique were carried out using an electrochemical workstation (CS350, Wuhan Corrtest Instruments Corp., Ltd., China) which equipped a conventional three-electrode cell containing steel rebar embedded in concrete, a Pt plate and a saturated-calomel-electrode as working electrode, the counter-electrode and reference-electrode, respectively. The EIS experiments were conducted at a frequency between 10^{-3} Hz and 10^{5} Hz. The polarization tests were performed at a scan rate of 1 mV/s and the cyclic voltammetric measurements were conducted at potential range from -1.0 V to 1.1 V at a scan rate of 30 mV/s after exposure time of 60 days.

3. RESULTS AND DISCUSSION

The polarization plots of carbon steel in different designs of mixtures specimens which exposed to 3.5wt% NaCl solution after 60 days are depicted in Figure 1. It is observed from Figure 1 that all anodic polarization curves in passive zones of steels indicated to formation the passive layers onto the surface of steel when they were exposed to a simulated aggressive marine environment [16, 17]. In addition, there is a notable move in corrosion potential toward the more positive potential that indicates that the change the concrete content can effectually retard the dissolution of anodic metal [18, 19]. In polarization studies, the passive current is a meaningful parameter due it can measure the corrosion resistance of the steel in the passive state [2]. As observed, OPC+WA30+BFS30 sample shows the most expansive passive region and the lowest passive current density that demonstrates the enhancement of a corrosion resistance in the steel under corrosive environment. That is attributed to the reaction of the SiO_2 present in the WA and BFS with calcium hydroxide created during the cement hydration process which results in the formation of calcium silicate hydrate (C-S-H) as an improvement factor in durability, stability and mechanical properties of concrete [20-22]. Table 4 shows the obtained values of corrosion potential (E_{Corr}) and corrosion current density (I_{Corr}) from the polarization plots in Figure 1. Corrosion level can be described into four levels proposed by Durar Network Specification [23]: very high corrosion for I_{Corr}>1.0 μA/cm^2, high corrosion for I_{Corr} to be 0.5 μA/cm^2 or I_{Corr}<1.0μA/cm^2, low corrosion aimed at 0.1μA/cm^2< I_{Corr}<0.5μA/cm^2, and passivity aimed at I_{Corr}<0.1μA/cm^2. As seen from Table 4, the corrosion current density of OPC+BFS60, OPC+WA60 and OPC+WA30+BFS30 samples in 3.5 wt% NaCl solution is lower than that of control sample, and indicated to passivity state [24, 25]. The lowest corrosion current density occurs in OPC+WA30+BFS30. Addition of alternative cementitious materials such as BFS and WA are added into concrete can decrease the porosity which reduces the permeability and improve the resistance of concrete to the penetration of harmful substances such as chloride and sulfate ions, carbon dioxide, water and oxygen, decrease the mobility of the corrosive ions and thereby the improve durability performance and enhance the corrosion resistance [26-28].

Furthermore, the values of cathodic and anodic Tafel slopes (βc, βa) are obtained by the linear extrapolation of the Tafel slopes [29, 30]. Table 4 shows the value of βa and βc varied with the change in replacement in concrete samples which can be related to inhibition behavior for carbon steel [31-33]. As seen, the anode Tafel slope of OPC+WA30+BFS30 sample shows the highest value. It indicates to

synergetic effect BFS and WA in concrete can enhance the steel rebar corrosion resistance into 3.5 wt% NaCl solution. Studies have been demonstrated that the Al_2O_3 and SiO_2 in BFS and WA can provide pozzolanic reactions [34, 35]. The Al_2O_3 and SiO_2 particles can fill smaller pores present in the mixture of cement and result more gaps being closed [36, 37]. The chemical effects of Al_2O_3 and SiO_2 particles include the enhancement of pozzolanic reaction which cause to formation and calcium aluminate hydrate (C-A-H) and C-S-H gels, respectively [38, 39]. These gels can serve as the nucleation sites to form a denser and stronger matrix [40-42]. In addition, addition WA can compensate the side effects of BFS on steel rebar corrosion resistance.

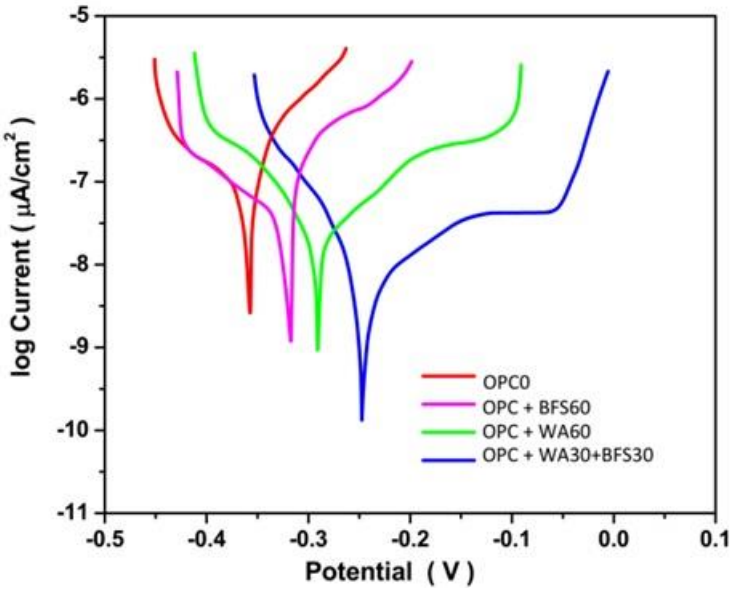

Figure 1. The polarization plots of carbon steel in different designs of mixtures specimens which exposed to 3.5wt% NaCl solution after exposure time of 60 days.

Table 4. The obtained data from the polarization plots.

Sample name	**Corrosion potential (V)**	**Corrosion current density(μA/cm²)**	**-β_a(mV/dec)**	**β_c(mV/dec)**
OPC0	-0.369	0.345	22	51
OPC + BFS60	-0.326	0.101	26	56
OPC + WA60	-0.281	0.077	33	57
OPC + WA30+BFS30	-0.245	0.033	35	53

The CV technique was employed for investigating the redox behavior and creation of the passive layer on the steel in the alkaline media. The CV curves of the specimens in 3.5 wt% NaCl solution are

shown in Figure 2 which reveals the redox peaks for all specimens containing anodic and cathodic peaks at the potential of 0.02 V and -0.31 V, respectively which is attributed to the following reactions based on oxidation Fe^{2+} into Fe^{3+} and formation of passive film on the steel surface [43, 44]:

$$Fe + 2OH^- \rightleftharpoons Fe(OH)_2 + 2e^- \quad (1)$$

$$3Fe(OH)_2 + 2OH^- \rightleftharpoons Fe_3O_4 + 4H_2O + 2e^- \quad (2)$$

$$3FeO + 2OH^- \rightleftharpoons Fe_3O_4 + 2e^- \quad (3)$$

As seen, the OPC+WA30+BFS30 sample shows the lowest current in CV curve that can be related to the formation of the stable passivation films onto the steel surface [45]. Moreover, the anodic current density sharply decreases for sweep the potential up to 0.6 V that it can be mainly associated with anodic oxygen evolution [46, 47]. In cathodic scan, when potential is moved to a further negative direction, the cathodic current is significantly increased, indicating to hydrogen evolution reaction becomes dominant [48, 49]. In addition, OPC+WA30+BFS30 sample shows the lowest anodic peak current toward the other samples that evidences the simultaneous existences of BFS and WA in OPC promotes corrosion resistance and makes more stable the formed passive film on the steel rebar surface.

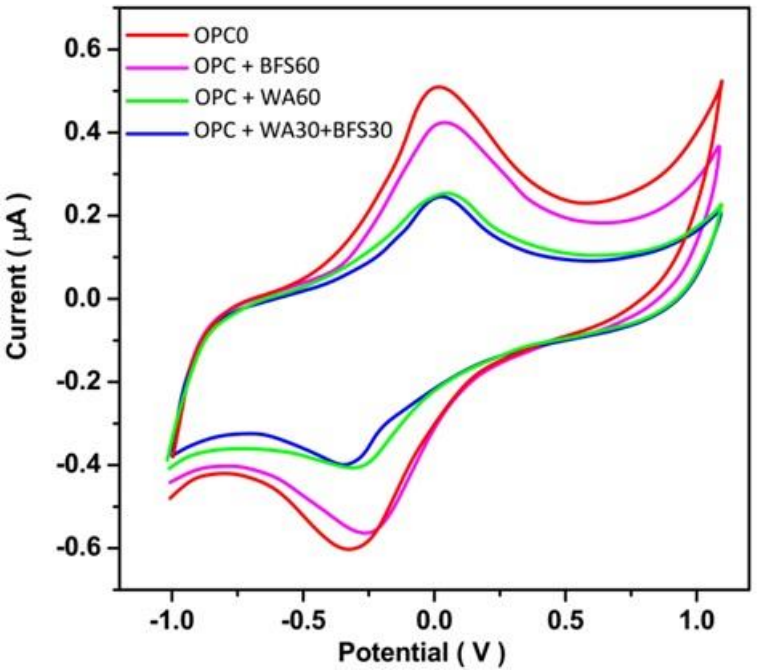

Figure 2. The CV curves of the specimens in 3.5 wt% NaCl solution after an exposure time of 60 days.

EIS analyses have been utilized to study the steel rebar corrosion resistance embedded in concretes with different design of replacement of admixtures at 3.5 wt% NaCl solution after an exposure time of 60 days. Figure 3 depicts the obtained Nyquist diagrams by the EIS technique and the corresponding equivalent circuit model which contained Rs as the resistance of solution, Q_1 as the double-layer capacitance of the steel surface, R_{ct} as charge transfer resistance, Q_2 as capacitance and R_c as the resistance element for coated concrete [50]. Table 5 shows the obtained data by modeling to the

equivalent circuit according with the Nyquist plots. As observed from the Table 5, OPC+WA30+BFS30 sample shows the highest values of R_C and R_{ct} and lowest values for Q_1 and Q_2, indicating to increase in the corrosion resistance and formation of stable and thick passive film on the steel rebar [51]. Studies indicated that the addition of WA in cement can act as activator and adds nucleation sites which facilitate the precipitation of additional hydrates [52, 53]. The addition of WA in the cement can decrease the amount of calcium oxide by decreasing $Ca(OH_2)$ with pozzolanic reaction, and changing it to secondary C─S─H gel which leads to enhancing the sulfate attack resistance in the concrete [54, 55]. In addition, the BFS can inhibit the calcium hydroxide growth due to great surface area for hydraulic reactions [56, 57]. The mineral admixtures as binders can fill small pores and voids harmful to the structure of concrete and offers a more robust structure and higher corrosion resistance of reinforcement steel bars in corrosive solutions [58].

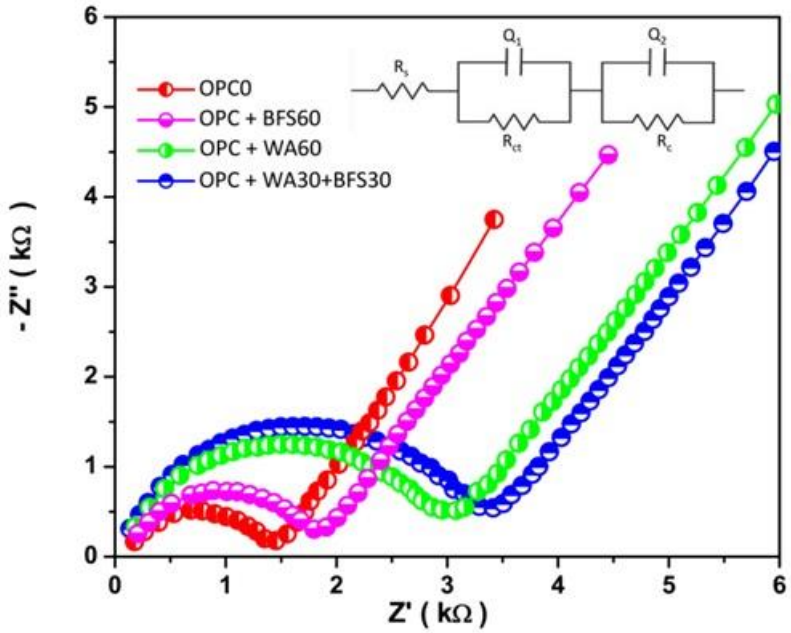

Figure 3. The obtained Nyquist diagrams by the EIS technique and the corresponding equivalent circuit models after an exposure time of 60 days.

Table 5. The obtained data by modeling with the equivalent circuit according with the Nyquist plots.

Sample	**R_s(Ω)**	**R_{ct} (kΩ)**	**Q_1 (μF/cm^2)**	**R_c (kΩ)**	**Q_2 (μF/cm^2)**
OPC0	12.3	1.519	7.6	0.869	5.2
OPC + BFS60	13.7	2.060	5.8	1.761	3.7
OPC + WA60	10.8	3.155	3.5	2.415	2.0
OPC + WA30+BFS30	11.7	3.538	1.9	2.799	1.7

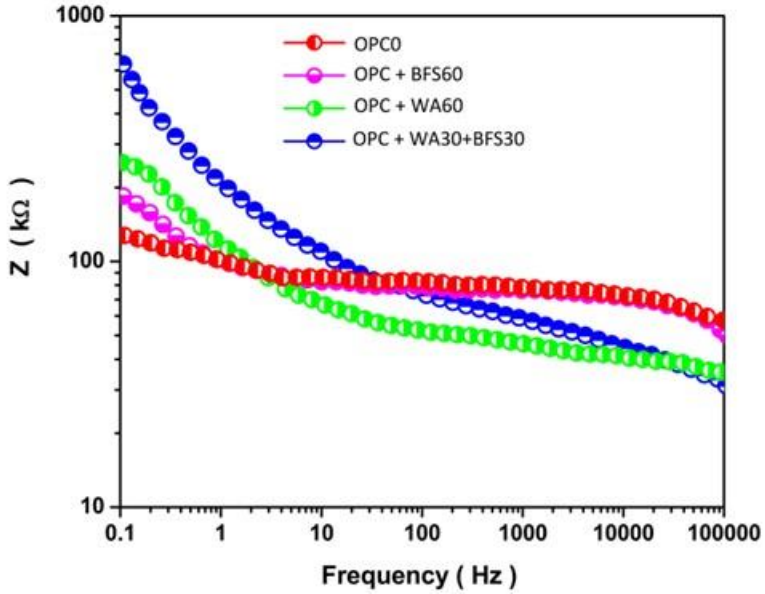

Figure 4. The obtained Bode plots from the EIS analyses after an exposure time of 60 days.

Moreover, results shows that the Q_2 value is lower than Q_1 in all samples, implying to high capacitive behavior of double layer [59]. Figure 4 shows the obtained Bode plots from the EIS analyses. As found, the OPC+WA30+BFS30 and then OPC+WA60 samples exhibit the appropriate effect to prevent the corrosion reactions into steel reinforced concretes. These findings are remarkably in agreement with the EIS results.

The SEM micrographs of steel reinforced in OPC+WA30+BFS30 and OPC0 specimens after immersing into 3.5 wt% NaCl media for 60 days are displayed in Figure 5. As can be seen, the OPC+WA30+BFS30 specimen exhibits lower corrosion products and a lower density of narrow pits on the steel surface than the OPC0 specimen, which exhibits mild pitting corrosion with small pinholes on the steel surface due to a decrease in corrosive ion permeability and mobility in the concrete [60]. The OPC0 specimen exhibits thick corrosion products and larger pits with inner rust, which is consistent with the results of the EIS analyses.

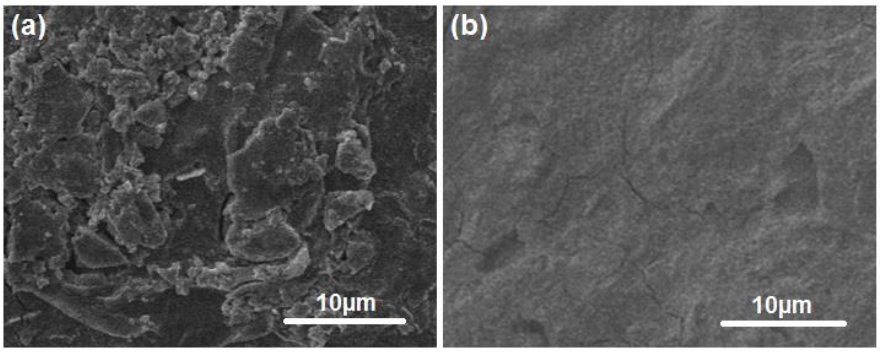

Figure 5. The SEM micrographs of steel reinforced in OPC0 and OPC+WA30+BFS30 specimens after immersing into 3.5 wt% NaCl media for 60 days.

4. CONCLUSION

This study was focused on the evaluation of corrosion resistance of ordinary Portland cement blended with WA and BFS as mineral admixtures in reinforced concrete under simulated marine conditions using electrochemical techniques. WA and BFS admixtures were used to partially replace the OPC included OPC+BFS60, OPC+WA60 and OPC+WA30+BFS30 samples. Results of potentiodynamic polarization, cyclic voltammetry and electrochemical impedance spectroscopy studies indicated that OPC+WA30+BFS30 sample showed higher corrosion resistance and potential than the other samples because of the synergetic effect BFS and WA in concrete which enhanced the steel rebar corrosion resistance into 3.5wt% NaCl media. Results showed that the Al_2O_3 and SiO_2 in BFS and WA can provide the pozzolanic reactions. Moreover, the SEM studies showed that the OPC+WA30+BFS30 had the lower corrosion products and lower density of narrow pits on steel surface than that OPC0 specimen which demonstrated mild pitting corrosion with small pinholes on the surface of steel because of decrease of corrosive ions permeability and mobility in the concrete which confirmed the electrochemical studies. These results demonstrated that WA and BFS can used as appropriate mineral admixtures to decrease hydroxide ion concentrations and enhance the passivation of the reinforcement steel rebar in marine environments.

References

1. S. Kakooei, H.M. Akil, A. Dolati and J. Rouhi, *Construction and Building Materials*, 35 (2012) 564.
2. W. Zhang and Y. Huang, *Construction and Building Materials*, 350 (2022) 128818.
3. N. Mohamed, M. Boulfiza and R. Evitts, *Journal of materials engineering and performance*, 22 (2013) 787.
4. E. Aprianti, *Journal of cleaner production*, 142 (2017) 4178.
5. T. Shi, Y. Liu, Y. Zhang, Y. Lan, Q. Zhao, Y. Zhao and H. Wang, *International Journal of Concrete Structures and Materials*, 16 (2022) 1.
6. X. Cui, C. Li, Y. Zhang, Z. Said, S. Debnath, S. Sharma, H.M. Ali, M. Yang, T. Gao and R. Li, *Journal of Manufacturing Processes*, 80 (2022) 273.
7. S. Kakooei, H.M. Akil, M. Jamshidi and J. Rouhi, *Construction and Building Materials*, 27 (2012) 73.
8. S. Wu, *Global Journal of Research In Engineering*, 19 (2019) 33.
9. E. Oziegbea, V. Olarewajub and O. Ocanc, *Malaysian Journal of Geosciences (MJG)*, 4 (2020) 13.
10. R. Sharma, J.G. Jang and P.P. Bansal, *Journal of Building Engineering*, 45 (2022) 103314.
11. C. Xupeng, S. Zhuowen and P. Jianyong, *Materials Research Express*, 8 (2021) 115506.
12. J. Sun, Z. Wang and Z. Chen, *Journal of Thermal Analysis and Calorimetry*, 131 (2018) 2291.
13. X. Wang, C. Li, Y. Zhang, H.M. Ali, S. Sharma, R. Li, M. Yang, Z. Said and X. Liu, *Tribology International*, 174 (2022) 107766.
14. B.S. Thomas, J. Yang, K.H. Mo, J.A. Abdalla, R.A. Hawileh and E. Ariyachandra, *Journal of Building Engineering*, 40 (2021) 102332.
15. T. Gao, Y. Zhang, C. Li, Y. Wang, Y. Chen, Q. An, S. Zhang, H.N. Li, H. Cao and H.M. Ali, *Frontiers of Mechanical Engineering*, 17 (2022) 1.
16. G. Blanco, A. Bautista and H. Takenouti, *Cement and Concrete Composites*, 28 (2006) 212.
17. M. Yang, C. Li, Y. Zhang, D. Jia, R. Li, Y. Hou, H. Cao and J. Wang, *Ceramics International*, 45 (2019) 14908.

18. S.-h. Shi and Y.-Q. Xiong, *International Journal of Electrochemical Science*, 16 (2021) 11644.
19. Y. Xie, S. Gao, Z. Ling, C. Lai, Y. Huang, J. Wang, C. Wang, F. Chu, F. Xu and M.-J. Dumont, *Journal of Materials Chemistry A*, 10 (2022) 13685.
20. D. Hou, J. Zhang, Z. Li and Y. Zhu, *Materials and structures*, 48 (2015) 3811.
21. F. Bellmann and J. Stark, *Cement and Concrete Research*, 39 (2009) 644.
22. W. Xu, C. LI, Y. Zhang, H.M. Ali, S. Sharma, R. Li, M. Yang, T. Gao, M. Liu and X. Wang, *International Journal of Extreme Manufacturing*, 4 (2022) 042003.
23. L. Fan, W. Meng, L. Teng and K.H. Khayat, *Composites Part B: Engineering*, 177 (2019) 107445.
24. Z. Zhang, G. Liang, Q. Niu, F. Wang, J. Chen, B. Zhao and L. Ke, *Quality and Reliability Engineering International*, 38 (2022) 3710.
25. N. Wang, R. Zhao, L. Zhang and X. Guan, *Microporous and Mesoporous Materials*, 345 (2022) 112248.
26. K. Hassan, J. Cabrera and R. Maliehe, *Cement and concrete composites*, 22 (2000) 267.
27. Y. Yang, Y. Gong, C. Li, X. Wen and J. Sun, *Journal of Materials Processing Technology*, 291 (2021) 117023.
28. B. Fan, X. Zhao, Z. Liu, Y. Xiang and X. Zheng, *Sustainable Chemistry and Pharmacy*, 29 (2022) 100821.
29. N. Hebbar, B. Praveen, B. Prasanna, T. Venkatesha and S. Abd Hamid, *Procedia Materials Science*, 5 (2014) 712.
30. W. Zheng, L. Yin, X. Chen, Z. Ma, S. Liu and B. Yang, *Pattern Recognition*, 120 (2021) 108153.
31. Y. Yang and W. Luo, *International Journal of Electrochemical Science*, 15 (2020) 12410.
32. X. Wang, C. Li, Y. Zhang, Z. Said, S. Debnath, S. Sharma, M. Yang and T. Gao, *The International Journal of Advanced Manufacturing Technology*, 119 (2022) 631.
33. S. Hou, B. Shen, D. Zhang, R. Li, X. Xu, K. Wang, C. Lai and Q. Yong, *Bioresource Technology*, 362 (2022) 127825.
34. K. Horii, T. Kato, K. Sugahara, N. Tsutsumi and Y. Kitano, *Nippon Steel & Sumitomo Technical Report*, 109 (2015) 5.
35. X. Zhang, C. Li, Y. Zhang, D. Jia, B. Li, Y. Wang, M. Yang, Y. Hou and X. Zhang, *The International Journal of Advanced Manufacturing Technology*, 86 (2016) 3427.
36. S.C. Paul, A.J. Babafemi and M.J. Miah, *Proceedings of the 6th World Congress on Civil, Structural, and Environmental Engineering (CSEE'21), Lisbon, Portugal*, 1 (2021) 21.
37. W. Zheng, X. Liu, X. Ni, L. Yin and B. Yang, *IEEE access*, 9 (2021) 91476.
38. N.H.A.S. Lim, H. Mohammadhosseini, M.M. Tahir, M. Samadi and A.R.M. Sam, *Arabian Journal for Science and Engineering*, 43 (2018) 5305.
39. J. Zhang, C. Li, Y. Zhang, M. Yang, D. Jia, G. Liu, Y. Hou, R. Li, N. Zhang and Q. Wu, *Journal of Cleaner Production*, 193 (2018) 236.
40. J.-W. Lee, Y.-I. Jang, W.-S. Park, S.-W. Kim and B.-J. Lee, *Materials*, 12 (2019) 1037.
41. Z. Duan, C. Li, W. Ding, Y. Zhang, M. Yang, T. Gao, H. Cao, X. Xu, D. Wang and C. Mao, *Chinese journal of mechanical engineering*, 34 (2021) 1.
42. B. Fang, Z. Hu, T. Shi, Y. Liu, X. Wang, D. Yang, K. Zhu, X. Zhao and Z. Zhao, *Ceramics International*, (2022) 1.
43. C. Andrade, M. Keddam, X. Nóvoa, M. Pérez, C. Rangel and H. Takenouti, *Electrochimica Acta*, 46 (2001) 3905.
44. S. Liu, C. Gao and P. Yan, *Int. J. Electrochem. Sci*, 15 (2020) 5333.
45. Y. Wang, X. Cheng and X. Li, *Electrochemistry Communications*, 57 (2015) 56.
46. M.D. Obradović, B.D. Balanč, U.Č. Lačnjevac and S.L. Gojković, *Journal of Electroanalytical Chemistry*, 881 (2021) 114944.
47. T. Gao, C. Li, M. Yang, Y. Zhang, D. Jia, W. Ding, S. Debnath, T. Yu, Z. Said and J. Wang, *Journal of Materials Processing Technology*, 290 (2021) 116976.
48. L. Niu and Y. Cheng, *Applied surface science*, 253 (2007) 8626.

49. M. Liu, C. Li, Y. Zhang, M. Yang, T. Gao, X. Cui, X. Wang, W. Xu, Z. Zhou and B. Liu, *Chinese Journal of Aeronautics*, (2022) 1.
50. P. Leuaa, D. Priyadarshani, D. Choudhury, R. Maurya and M. Neergat, *RSC advances*, 10 (2020) 30887.
51. W. Yujie, Z. Huiwen and F. Xu, *International Journal of Electrochemical Science*, 17 (2022) 220348.
52. A. Qudoos, E. Kakar, A.u. Rehman, I.K. Jeon and H.G. Kim, *Applied Sciences*, 10 (2020) 3511.
53. K. Wang, S. Gao, C. Lai, Y. Xie, Y. Sun, J. Wang, C. Wang, Q. Yong, F. Chu and D. Zhang, *Industrial Crops and Products*, 187 (2022) 115366.
54. H.Ş. Arel and B.S. Thomas, *Results in physics*, 7 (2017) 843.
55. W. Zheng, X. Liu and L. Yin, *Applied Sciences*, 11 (2021) 1316.
56. C.M. Yun, M.R. Rahman, C.Y.W. Phing, A.W.M. Chie and M.K.B. Bakri, *Construction and Building Materials*, 260 (2020) 120622.
57. A. Mohammad and E. Dhanamjayarao, *Malaysian Journal of Geosciences*, 5 (2021) 12.
58. E. Güneyisi, M. Gesoğlu, S. Karaoğlu and K. Mermerdaş, *Construction and Building Materials*, 34 (2012) 120.
59. B. Li, Y. Huan and W. Zhang, *International Journal of Electrochemical Science*, 12 (2017) 10402.
60. J. Wei, R. Chen, W. Huang, X. Bian and B. Chen, *Construction and Building Materials*, 321 (2022) 126402